CHALMERS | UNIVERSITY OF GOTHENBURG

PREPRINT 2010:42

Models for road surface roughness

KLAS BOGSJÖ
KRZYSZTOF PODGÓRSKI
IGOR RYCHLIK

Department of Mathematical Sciences
Division of Mathematical Statistics
CHALMERS UNIVERSITY OF TECHNOLOGY
UNIVERSITY OF GOTHENBURG
Gothenburg Sweden 2010

Preprint 2010:42

Models for road surface roughness

Klas Bogsjö, Krzysztof Podgórski and Igor Rychlik

Department of Mathematical Sciences
Division of Mathematical Statistics
Chalmers University of Technology and University of Gothenburg
SE-412 96 Gothenburg, Sweden
Gothenburg, September 2010

Preprint 2010:42
ISSN 1652-9715

Matematiska vetenskaper
Göteborg 2010

Models for road surface roughness

KLAS BOGSJÖ*, KRZYSZTOF PODGÓRSKI** AND IGOR RYCHLIK***
Adresses:
* Scania CV AB, RTRA Load Analysis, SE-15187 Sdertlje, Sweden
klas.bogsjo@scania.com
** Mathematical Statistics, Centre for Mathematical Sciences, Lund University, Box 118, 221 00 Lund, Sweden
krys@maths.lth.se
*** Mathematical Sciences, Chalmers University of Technology, SE-412 96 Gteborg, Sweden (Corresponding author)
rychlik@chalmers.se

Abstract

Road sections with high degree of roughness are of special interest, since these have a significant impact on vehicle's fatigue life. The study is focused on statistical description and analysis of road surface irregularities essential for heavy vehicle fatigue assessment. The Laplace moving average process is proposed to model the surface. It is compared with the model proposed in [6] that models a road surface as a homogenous Gaussian process with MIRA spectrum with added randomly placed and shaped irregularities. A hybrid model that combines the two models is also given. The models are fitted to 8 measured road surfaces. The accuracy of the models is discussed.

Keywords: Road surface irregularity, damage variability, Laplace moving averages, MIRA spectrum.

1 Introduction

This paper presents comparison between different means to model the roughness of road surface. The methods are compared on eight measured roads of total length about 230 km. The measured roads are of varying quality, ranging from rough gravel and asphalt roads from the north of Sweden to smooth asphalt roads from the south of Sweden. The signals have different lengths and are scaled to have variance one and zero mean. Models are intended to be used in fatigue damage prediction of vehicle components and hence the most important property of the model is its capacity to describe variability of stresses in a vehicle. This is evaluated by employing a "fatigue filter" to the measured/simulated road surfaces; i.e. by estimating a response of a simple model for a truck and comparing the rainflow damage, see [14], of the responses.

Fatigue damage is assessed by studying a quarter-vehicle model traveling at constant velocity on road profiles, see Figure 1. This very simple model cannot be expected to predict loads on a physical vehicle exactly, but it will high-light the most important road characteristics as far as fatigue damage accumulation is concerned. The parameters in the model are set to mimic heavy vehicle dynamics. The response is the total force acting on the sprung mass is denoted $Y(t)$.

Neglecting the possible "jumps", i.e. that a vehicle can loose constant with the road surface, the response can be estimated by means of linear filtering of the encountered road surface. The filter has the following transfer function

$$H(\omega) = \frac{m_s\omega^2(k_t + i\omega c_t)}{k_t - \frac{(k_s+i\omega c_s)\omega^2 m_s}{-m_s\omega^2+k_s+i\omega c_s} - m_u\omega^2 + i\omega c_t}\left(1 + \frac{m_s\omega^2}{k_s - m_s\omega^2 + i\omega c_s}\right). \tag{1}$$

Assuming that the road is stationary with power spectral density $S_Z(f)$, where f is the wave number having units m^{-1}, then the response Y, for a vehicle at speed v [m/s], has power spectral density given by

$$S_Y(\omega) = \frac{1}{v}|H(\omega)|^2 S_Z\left(\omega/(2\pi v)\right).$$

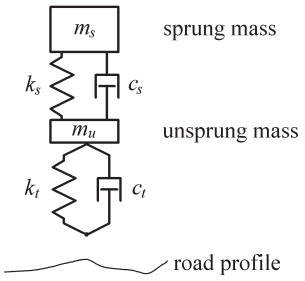

Symbol	Value	Unit
m_s	3400	kg
k_s	270 000	N/m
c_s	6000	Ns/m
m_u	350	kg
k_t	950000	N/m
c_t	300	Ns/m

Figure 1: Quarter vehicle model

The vertical road variability consists of slowly changing landscape and the road surface irregularity (roughness). Often one assumes that energy of $S_Z(f)$ for frequencies $f < 0.01$ m^{-1} (wavelengths above 100 meters) represents landscape variability which does not affect the vehicle dynamics and hence can be removed from the spectrum $S_Z(f)$. Similarly high frequencies $f > 10\,\mathrm{m}^{-1}$ (wavelengths below 10 cm) are filtered out by tire and also are removed from the spectrum.

Commonly, stochastic models are used to describe the randomness of measured road profiles. Vehicle models traveling on road profiles modeled as stationary Gaussian processes have been extensively studied (see for example [15] and [12] for some recent studies). However, measured profiles are not accurately described by a stationary Gaussian model. The reason is that the actual roads contain short sections with above-average irregularity. As shown in [6] such irregularities cause most of the vehicle fatigue damage.

In this paper three models will be compared. The first one is a non-homogenous Gaussian process, proposed in [6], the second is a homogenous Laplace Moving Average (LMA) process and the third one is a combination of the Gaussian and LMA processes which we will call the hybrid model. For visual comparison, a sample from each model is presented in Figure 2 and compared with the actual road record. The models are presented in the following three sections. In the last section they will be applied to describe variability observed in 8 measured road surfaces of total length of about 230 km. Accuracy of the models is discussed in that section as well.

2 Non-homogenous Gaussian model

In the model that was first presented in [6], one assumes in the road records two types of waves: short ones with wavelengths between 5 and 0.1 meters and long ones with wavelengths between 100 and 5 meters. The main variability in the road is described by homogenous independent Gaussian processes: $Z_0^{(1)}(t)$ for long waves and $Z_0^{(2)}(t)$ for short waves. Their corresponding spectra for long waves $S_0^{(1)}(f) = 10^{a_0}\,(f/f_0)^{-w_1}$, $f \in [0.01, 0.20]$, and for short waves $S_0^{(2)}(f) = 10^{a_0}\,(f/f_0)^{-w_2}$, $f \in [0.2, 10]$, where f is the wave number having units m^{-1}. These spectra when put together give the so called MIRA spectrum, see [9], viz.

$$S_0(f) \;=\; \begin{cases} 10^{a_0}\left(\frac{f}{f_0}\right)^{-w_1}, & f \in [0.01, 0.20], \\ 10^{a_0}\left(\frac{f}{f_0}\right)^{-w_2}, & f \in [0.20, 10], \\ 0, & \text{otherwise,} \end{cases} \quad , \tag{2}$$

where $f_0 = 0.2$. Here, as suggested in [8], 10^{a_0} is the basic roughness coefficient. The exponent w_1 describe energy distribution between components of wavelengths between 100 and 5 meters, while w_2, wavelengths between 5 and 0.1 meters describes state of road deterioration.

As mentioned above measured road tracks contain short sections with above-average irregularity which cause most of the vehicle fatigue damage. It was found that these irregularities occur both for

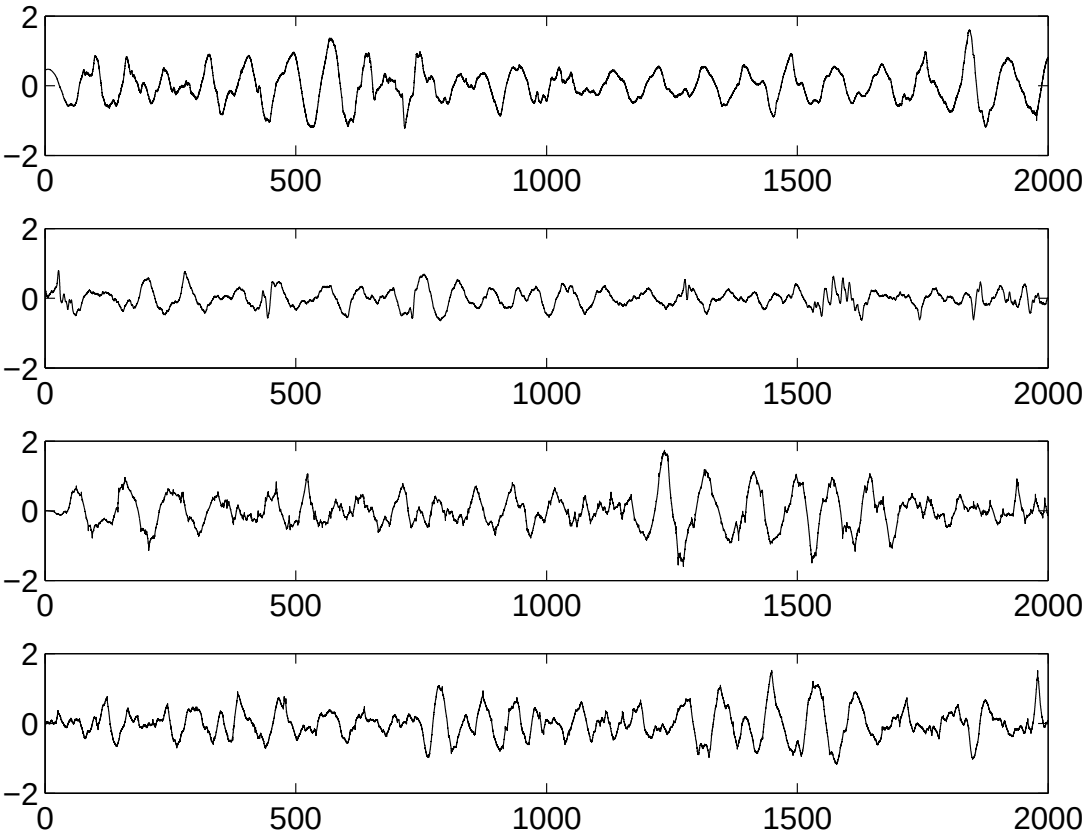

Figure 2: An actual record taken from $2km$ road section (*Top*) and the model generated samples from fits to this record: Non-homogenous Gaussian (*second top*), Laplace moving average (*third top*), and the hybrid model (*bottom*).

long and short waves. In [8] it is noted that "As a road's state of repair deteriorates, a decrease in the exponent w_2 is to be anticipated", i.e. short wave irregularities are created or change their shapes. In the non-homogenous Gaussian model the irregularities are accounted by adding to Gaussian processes $Z_0^{(1)}(x)$ and $Z_0^{(2)}(x)$ long and short wave irregularities $Z_i^{(1)}(x)$, $Z_i^{(2)}(x)$, $i > 0$, of random shape, length and location. The road with superimposed irregularities is denoted by $Z(x)$ and given by

$$Z(x) = \sum_{i=0}^{N_1} Z_i^{(1)}(x) + \sum_{i=0}^{N_2} Z_i^{(2)}(x), \tag{3}$$

where N_1, N_2 are (random) number depending on the length of the road while the processes $Z_i^{(1)}(x)$, $Z_i^{(2)}(x)$, $i = 0, 1, \ldots$, are mutually independent.

To avoid discontinuities at the start and end of the rough sections, the added irregularities starts and ends with zero slope and zero level, see [5] for more details. Furthermore, the location and length of the sections with added roughness are random. More precisely, the distance between the end of an irregularity and the start of the next is exponentially distributed. The irregularity length is also exponentially distributed. The long waves and short waves irregularities are added independently. The model requires knowledge of 9 parameters. For illustration, a 500 m long road is simulated and plotted in Figure 3. Some details of the simulation algorithm and form of $Z_i^{(k)}$'s are given in the appendix.

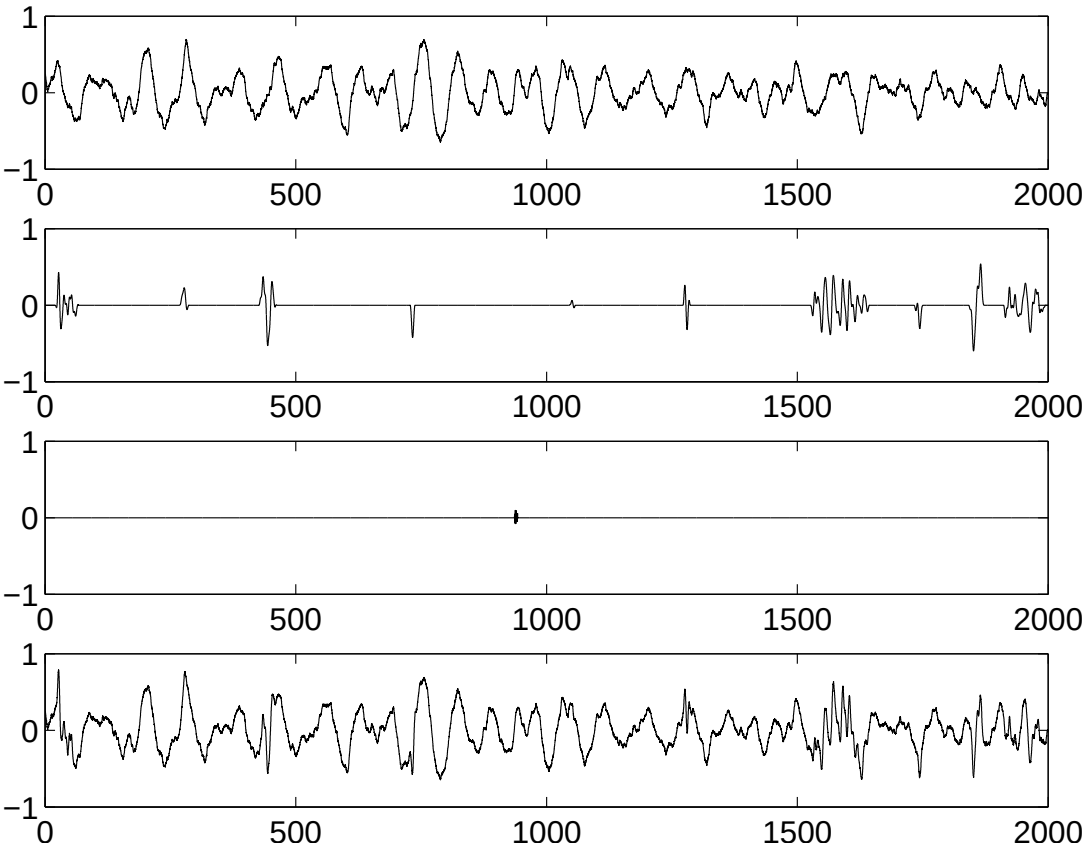

Figure 3: A synthetic (computer simulated) road profile $Z(x)$, defined by (3), lowest plot, the same as in Figure 2-*second top*. The first plot is the Gaussian process $Z_0(x)$, the second presents a sum of five long wave irregularities while the third a sum of short wave irregularities.

3 Laplace moving average model

Roughly speaking a moving average process is a convolution of a kernel function $f(x)$, say with, a infinitesimal "white noise" process having variance $d\,x$. Through the rest of the paper we assume that the kernel f is normalized so that its square integrates to one. For example, the Gaussian moving average (GMA) with mean zero and variance one can be written as

$$Z(x) = \int f(x-u)\, dB(u) \approx \sum f(x-x_i) Z_i \sqrt{d\,x}, \tag{4}$$

where $B(x)$ is Brownian motion, Z_i are independent standard Gaussian variables, while $d\,x$ is the discretization step, i.e. $\Delta B(x_i) = B(x_i + d\,x) - B(x_i) = \sqrt{d\,x} Z_i$, where Z_i's are standard normal variables. If $dB(u)$ or Z_i are no longer required to be normally distributed, one obtains moving average processes with non-Gaussian distributions. In this work, we are interested in the case when $Z_i\sqrt{dx}$ is replaced by $Z_i\sqrt{\nu\Gamma_i}$ where Γ_i is a gamma distributed with shape parametere dx/ν and scale one, so that $\mathsf{V}\left[Z_i\sqrt{\nu\Gamma_i}\right] = dx$. In this model the increments are Laplace distributed and thus leading to a Laplace moving average (LMA) given by

$$Z(x) = \int f(x-u)\, d\,\Lambda(u), \tag{5}$$

where $\Lambda(x)$ is the Laplace motion, cf. [1].

The process $Z(x)$ is symmetric around zero and the excess of kurtosis is $\kappa = 3\nu \int f^4(x)\,dx$. The parameter ν in Laplace motion $\Lambda(x)$ can be effectively estimated using the method of moments that is discussed in detail in [11]. Namely, if $\widehat{\kappa}$ is the sample excess kurtosis, then if $\widehat{\kappa} > 0$:

$$\widehat{\nu} = \frac{\widehat{\kappa}}{3\int f^4(x)\,dx}, \tag{6}$$

and zero otherwise. Note that $\kappa = \nu = 0$ corresponds to the limiting case of Gaussian moving average process, since as ν tends to zero $Z(x)$ becomes a GMA process.

A LMA (5) normalized so that it has mean zero and variance one is defined by its fourth moment and the kernel function f. Estimation of the kernel is not an easy task in general but for symmetric kernels it reduces to estimation of the covariance function or spectrum of the process. Namely, if the kernel is symmetric $f(-x) = f(x)$, i.e. the road profile characteristics do not depend on the direction one is driving on a road, then the spectrum $S_Z(\omega)$ of $Z(x)$ defines uniquely the kernel f since

$$S_Z(\omega) = \frac{1}{2\pi}|\mathcal{F}f(\omega)|^2,$$

where $\mathcal{F}$ stands the Fourier transform, and for symmetric kernels their Fourier transform is given by

$$\mathcal{F}f(\omega) = \sqrt{2\pi\, S_Z(\omega)}. \tag{7}$$

The simplest and most straightforward way of simulating a LMA is to first simulate the increments of the Laplace motion over an equally spaced grid and then to convolve them with the kernel $f(\cdot)$ as described next.

Increment based convolution algorithm for simulation of LMA

1. Pick m, and $\mathrm{d}x$ so that $f(\cdot)$ is well approximated by its values on
$$-m\,\mathrm{d}x < \ldots < -\mathrm{d}x < 0 < \mathrm{d}x < \cdots < m\,\mathrm{d}x.$$
2. Pick $n \gg 2m+1$ in order to simulate the $n-2m$ values of the LMA process Z at frequency $\mathrm{d}x^{-1}$.
3. Simulate n identically and independently distributed (i.i.d.) $\Gamma(\mathrm{d}x/\nu, 1)$ random variables and store them in a vector $G = [G_i]$.
4. Simulate n i.i.d. zero mean standard normal random variables and store them in a vector X.
5. Compute $Y = f * (\sqrt{\nu\, G}\cdot X)$, where $\sqrt{\nu\, G}\cdot X = [\sqrt{\nu\, G_i}\cdot X_i]$, where $*$ denotes the operation of convolution and the simulated $n-2m$ values of $\int f(x-u)\,d\,\Lambda(u)$ are obtained from Y by discarding its first and last m values.

4 The hybrid model

In practice Gaussian modeling is often used to model "undamaged" road surface to which one is adding potholes and other type irregularities. Since such an approach is physically appealing, we propose to alter the LMA model so that it will resemble this general scheme.

More precisely, the normalized (mean zero, variance one) road profile $Z(x)$ is written in the form

$$Z(x) = pZ_0(x) + \sum_{i=1}^{N} Z_i(x), p \in [0,1], \tag{8}$$

where $Z_0(x)$ is the zero mean variance one Gaussian process having spectrum S_Z, while $Z_i(x)$'s are taken from a jump process representation of LMA described in the Appendix, Eq. (12).

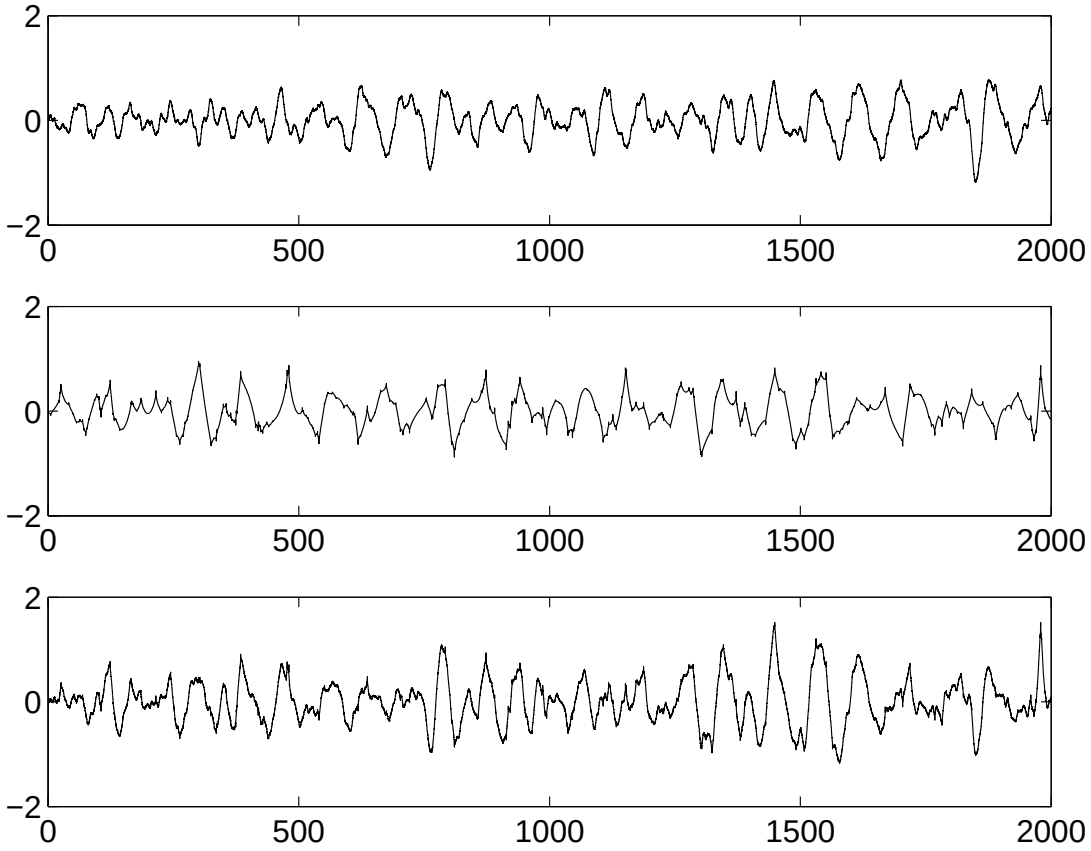

Figure 4: *Top:* Gaussian component $pZ_0(x)$, $p = 0.75$, of the hybrid model; *Middle:* "irregular" component $\sum_{i=1}^{N} Z_i(x)$; *Bottom:* the hybrid model which is the sum of the two – this is the same as in Figure 2 bottom.

The kernel function f used in $Z_i(x)$, $i \geq 1$ is computed using (7), while S_Z used in $Z_0(x)$ is chosen to be MIRA spectrum (2), defined by three parameters w_1, w_2 and a_0. One can interpret w_1 as the long wave irregularity of the road while w_2 reflects the state of deterioration of the road surface. The parameter a_0 is chosen in such a way that the zero order spectral moment of S_Z is one, i.e. $2\pi \int_0^\infty S_Z(f)\, df = 1$.

The parameter p in (8) can be used to define N. Namely, from the Appendix, Eq. (13) we have

$$\mathsf{V}\left[\sum_{i=1}^{N} Z_i(x)\right] \approx 1 - e^{-N\nu/L}.$$

Hence

$$N \approx -2\frac{L}{\nu}\ln p.$$

The "added" irregularities has the shape of the kernel function f which which contains both long- and short- wave component. The locations of irregularities are uniformly distributed over the interval $[0, L]$. The amplitude is random. Note that 4 parameters are needed to define the hybrid model (not counting the mean and standard deviation that have to be used for normalization), while the non-homogenous Gaussian model, presented in Section 2, requires 9 parameters. In Figure 4, a simulation of the hybrid method with $p = 0.75$ is shown. The algorithm that has been used for this purpose is presented next.

Convolution algorithm for simulation of $\sum_{i=1}^{N} Z_i(x)$ in (8).

1. Pick $\mathrm{d}x$ so that $f(\cdot)$ is well approximated by its values on
$$-m\mathrm{d}x < \ldots < -\mathrm{d}x < 0 < \mathrm{d}x < \cdots < m\,\mathrm{d}x.$$
2. Pick $n \gg 2m+1$ in order to simulate the $n-2m$ values of the LMA process Z at the points at frequency $\mathrm{d}x^{-1}$.
3. Pick $N \ll n$ and simulate N identically and independently distributed variables W_i, G_i. Compute $\gamma_i = \sum_{j=1}^{i} G_j$ and store variables in two vectors vector $\gamma = [\gamma_i]$, $W = [W_i]$.
4. Simulate N independent standard normal random variables X_i and store them in a vector X.
5. Compute a vector $R = \sqrt{\nu}\, X \cdot \left(e^{-\nu\gamma/L} W\right)^{1/2}$, where $R_i = \sqrt{\nu}\, X_i \cdot \left(e^{-\nu\gamma_i/L} W_i\right)^{1/2}$.
6. Choose at random N indexes $1 \le k_i \le n$ and define a vector Q of length n, such that $Q_{k_i} = R_i$) and zero otherwise.
7. Compute $Y = f * Q$, where $*$ denotes convolution and the simulated $n-2m$ values of $\sum_{i=1}^{N} Z_i(x)$ are obtained from Y by discarding its first and last m values.

5 Comparisons of the models

In this section we shall employ the three models to estimate the pseudo-damage of the response Y. The estimation procedure is based on eight measured road surfaces with the total length is about 230 km. Once the models are fitted to the data the damages they induce are evaluated. These damages relative to the damage inflicted by the actual road record will be used to compare the accuracy of the proposed models.

As discussed in the work [3] one needs more than 100 km of homogenous record to have the statistical uncertainty of the estimated damage to be negligible. The measurements are about 29 km long in average and hence statistical errors in the damage estimation are not negligible. However long records are often non homogenous which introduces bias (modeling error). Therefore the choice of the record length is the trade off between the size of the statistical uncertainties in the estimated parameters and the possible modeling errors. The life length of components is of order 10^5 km. It is strongly correlated to the sum of the pseudo damages accumulated during the usage of a vehicle hence it is desirable that the estimation of the damages is unbiased. This is because the coefficient of variation of the accumulated damage decreases as the inverse square root of the driven distance and often can be neglected relatively to the other sources of uncertainties, e.g. the driver behavior, material properties, geometry of components. Consequently the accumulated damage can be approximated by the expected damage which is proper as long as the latter is not heavily biased, see e.g. [3] for more detailed discussion.

Our approach to bias reduction is through considering shorter fragments of roads for which it maybe reasonable to assume homogeneity (constant values of parameters) of the models. Then the models are fitted for each fragment separately. Two different record lengths will be used. First we just consider the original eight measured records. Obviously shorter records are always possible to define by simply dividing measurements into shorter blocks. We create the second set of blocks by dividing the eight records into 5 km long road segments. In this case there will be 44 shorter records in total and the three models are fitted to each of them.

5.1 Estimation of relative damage

For a measured or simulated road surface Z the response $Y(t)$ is computed by means of filtering the signals $Z(v\,t)$, v is the vehicle speed, using the filter with transfer function $H(\omega)$ given in (1). In

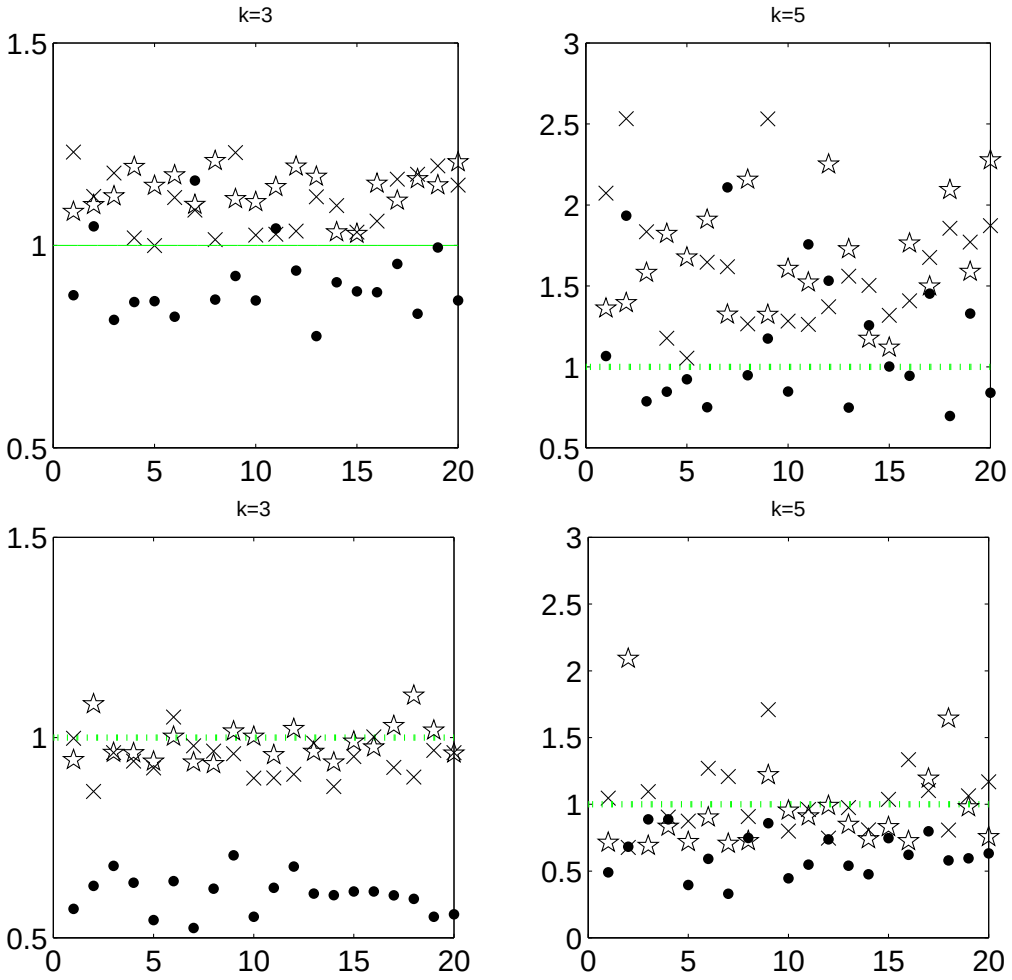

Figure 5: Twenty simulated relative damages (9) for 230 km long road profile, the vehicle speed is 15 m/s; stars D_k^{hybr}, crosses D_k^{LMA} and dots D_k^{nG}. *Left:* $k = 3$; *Right:* $k = 5$. *Top:* The three models were fitted to the eight measured road blocks; *Bottom:* The three models were fitted to 44 (each 5 km long) measured road fragments.

the example $v = 15$, and 10 m/s. The response of quarter vehicle $Y(t)$ is a solution of an 4th order ordinary differential equation. Since the initial conditions of the system at $t = 0$ are unknown the Hanning window has been used to make the start and the end of the ride smooth. This is necessary or otherwise the first oscillation of the response may cause all damage – the car is hitting a wall. Responses for measured and simulated roads are then computed using the FFT algorithm. Rainflow ranges h_i^{rfc} in the signal have been found has been found and the pseudo damage computed according to

$$D_k(Z) = \sum (h_i^{rfc})^k,$$

see [13] for details of this approach. Two values of k, 3 and 5, has been used. The damage D_k for higher exponent value $k = 5$ depends mostly on proportion and size of large cycles, while damage for $k = 3$, corresponding to crack growth process, depends on sizes of both large and moderately large cycles.

The pseudo-damage is computed for the observed road surface Z^{obs}, and simulated; Z^{nG} for non-Gaussian model, Z^{LMA} for symmetrical LMA road and Z^{hybr} for the hybrid model. The three relative

damages are defined by

$$D_k^{nG} = \frac{D(Z^{nG})}{D(Z^{obs})}, \quad D_k^{LMA} = \frac{D(Z^{LMA})}{D(Z^{obs})}, \quad D_k^{hybr} = \frac{D(Z^{hybr})}{D(Z^{obs})}. \tag{9}$$

A model is rejected if the relative damage values are significantly different from the value one.

5.2 Results

In this example about 230 km long measured road surface is used to compare the three proposed models. First we are using the eight consecutive measurements of different lengths. Since some of the roads are quite rough the speed v of 15 m/s could be considered as a rather high one. For the eight responses Y the damages were computed and summed to give the total damage accumulated for the 230 km long drive. Twenty independent simulations of the total damages have been computed and the relative damages (9) evaluated for two values of fatigue exponent $k = 3$ and $k = 5$. The results are presented in Figure 5, where stars denote D_k^{hybr}, crosses D_k^{LMA} and dots D_k^{nG}. One can see that the the data does not lead to rejection of the models. The LMA and hybrid model seems to give equivalent results. The most important statistical characteristics of the relative damages are given in Table 5.2 *(Left)*, where means and coefficients of variation are given. We note that the non-homogenous Gaussian model is closest to the observed damages. The model requires 9 parameters and some of them are not easy to estimate and require long measuring records. On the other hand, longer records are more non-homogenous in the parameters. Thus it may be harder to fit it with a single LMA or hybrid model.

Consequently, shorter records of 5 km, leading to 44 models have also been used. The resulting relative damage is presented in Figure 5 *(Bottom)*. Now one can see that non-homogenous Gaussian model give significantly too small damages, see also Table 5.2 *(Right)*, while both the LMA and hybrid model fits damages excellently.

Finally, since for some road surfaces the speed $v = 15$ m/s is rather high we give for completeness plots of the accumulated damages for a lower speed of 10 m/s. The plots in Figure 5 and Figure 6 are very similar. These indicate that the LMA and hybrid models perform similarly for a range of speed. Both are slightly conservative when only 8 longer records are used for estimation and work exceptionally well when 44 shorter records were used for model estimation.

6 Conclusions

Three models for vertical surface irregularity have been proposed. Comparing to actual road surface data all three models give satisfactory predictions of relative damages. The non-homogenous Gaussian model seems to work very well when enough data is available for estimation. The estimation employs quite complex algorithm described in [6]. The LMA and hybrid models are equivalent, although the LMA model uses empirical spectrum while the hybrid model uses the MIRA spectrum. Both models are somewhat conservative, which is advantageous but requires the accurate estimate of the spectrum

	k=3		k=5	
method	mean	c.v.	mean	c.v.
D_k^{LMA}	1.10	0.07	1.63	0.25
D_k^{nG}	0.91	0.10	1.15	0.36
D_k^{hybr}	1.14	0.05	1.66	0.21

	k=3		k=5	
method	mean	c.v.	mean	c.v.
D_k^{LMA}	0.95	0.05	1.03	0.23
D_k^{nG}	0.63	0.63	0.7	0.27
D_k^{hybr}	0.99	0.05	0.96	0.37

Table 1: Mean and coefficient of variation for the relative damages estimated using twenty simulated data presented in: Figure 5 *(Top)* – the left hand side table; Figure 5 *(Bottom)* – the right hand side table.

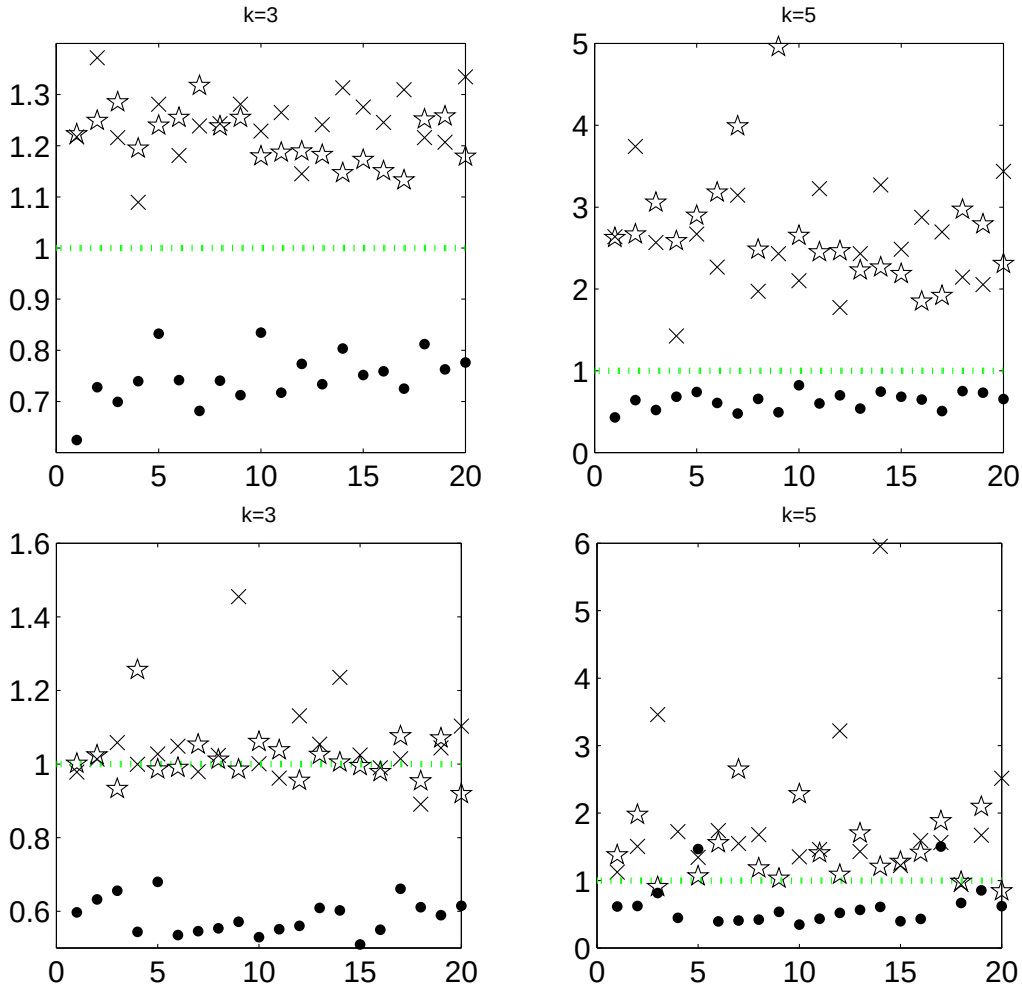

Figure 6: Twenty simulated relative damages (9) for 230 km long road profile; stars D_k^{hybr}, crosses D_k^{LMA} and dots D_k^{nG}. The vehicle speed is 10 m/s. *Left:* $k = 3$; *Right:* $k = 5$. *Top:* The three models were fitted to the eight measured road blocks; *Bottom:* The three models were fitted to the 44 each 5 km long measured road blocks.

to evaluate the kernel function. Finally, the hybrid model seems to work very well when fitted to short (homogenous) records. It requires only estimates of five parameters (essentially four since the last one, p or N, can be arbitrarily set to some low, large value, respectively, e.g. in examples $p = 0.75$ were used) which is convenient when one needs to describe the damage variability for longer road records. The local damage accumulated during 5 to 10 km computed by means of the hybrid model can then be averaged using long term distributions of parameters.

7 Acknowledgements

We thankful SCANIA for providing the measured road records. The Swedish foundation for Strategic Research through GMMC, Gothenburg Mathematical Modelling Center is acknowledge for support. Research of the second author partially supported by the Swedish Research Council Grant 2008-5382.

References

[1] Åberg, S., Podgórski K. (2010) A class of non-Gaussian second order random fields. *Extremes*, in print, DOI: 10.1007/s10687-010-0119-1.

[2] Åberg, S., Podgórski, K., and Rychlik, I. (2009) Fatigue damage assessment for a spectral model of non-Gaussian random loads. *Prob. Eng. Mech*, Vol 24, pp. 608-617.

[3] Bengtsson A., K., Bogsjö, K and Rychlik, I. (2009) Fatigue Damage Uncertainty pp. 151-171, chapter in *Robust Design Methodology for Reliability*, Wiley.

[4] Bogsjö K and Rychlik I. Vehicle fatigue damage caused by road irregularities. *Fatigue and Fracture of Engineering Materials and Structures*, Vol. **32**, pp. 391-402.

[5] Bogsjö K. (2006) Development of analysis tools and stochastic models of road profiles regarding their influence on heavy vehicle fatigue. *Suppl. Vehicle System Dynamics*, Vol. **44**, pp. 780–790.

[6] Bogsjö K. (2007) *Road profile statistics relevant for vehicle fatigue* PhD thesis, Univ. Lund, Dept. Mathematical Statistics.

[7] Bondesson, L. (1982) On simulation from infinitely divisible distributions. *Adv. Appl. Prob.* Vol. **14**, pp. 855-869.

[8] Dodds, C.J. and Robson, J.D. (1973) The description of road surface roughness *Journal of Sound and Vibration* Vol. **31**, pp. 175-183.

[9] Labarre, R. P., Forbes, R. T., Andrew, S. (1969) The measurement and analysis of road surface roughness. *Motor Industry Research Association Report*, No. 1970/5. .

[10] Kotz, S., Kozubowski, T.J., Podgórski, K. (2001) *The Laplace distribution and generalizations: A revisit with applications to communications, economics, engineering and finance.* Birkhaüser, Boston.

[11] Podgórski, K., Wegener, J. (2010) Estimation for stochastic models driven by Laplace motion. to appear in *Communications in Statistics: Theory and Methods*.

[12] Mucka P. (2004) Road waviness and the dynamic tyre force. *Int. J. Vehicle Design*, Vol. **36**, pp. 216–232,

[13] Rychlik, I. (1987) A new definition of the rainflow cycle counting method. *Int. J. Fatigue* **9**, 119-121

[14] (1993) Rychlik, I. Note on cycle counts in irregular loads. *Fatigue and Fracture of Engineering Materials and Structures*, Vo. **16**, pp. 377–390.

[15] Sun L. (2001) Computer simulation and field measurement of dynamic pavement loading. *Mathematics and Computers in Simulation*, Vol **56**, pp. 297–313, 2001.

Appendix:

Non-homogenous Gaussian model

In the measured road profile sections rougher than normal parts are identified. The parts are classified as long wave and short wave irregularities. The parameters used for description of the long- short-

wave irregularity will be $i = 1, 2$, respectively. From the two sequences (long-, short-irregularities) two spectrums are estimated

$$S_1(f) = \begin{cases} (10^{a_1} - 10^{a_0}) \left(\frac{f}{f_0}\right)^{-w_1}, & f \in [0.01, 0.20], \\ 0, & \text{otherwise,} \end{cases}, \tag{10}$$

$$S_2(f) = \begin{cases} (10^{a_2} - 10^{a_0}) \left(\frac{f}{f_0}\right)^{-w_2}, & f \in [0.20, 10], \\ 0, & \text{otherwise,} \end{cases}. \tag{11}$$

Next for the spectrums the corresponding covariance functions $r_1(x)$, $r_2(x)$, say, are computed. The expected lengths θ_i, $i = 1, 2$, of rougher parts are estimated and the average distances between the end of an irregularity and the beginning of the next μ_i are found. Here the average distance between the irregularities is $\mu_i + \theta_i$. We turn next to simulation algorithm of the non-homogenous Gaussian road roughness model.

Simulation of non-homogenous Gaussian profile of length L

1. Simulate a homogenous Gaussian process $Z_0(x)$, $0 \le x \le L$, with spectrum S_0.

2. Simulate n_1 independent exponentially distributed variables U_i, V_i having average values μ_1, θ_1, respectively, and evaluate $X_i = \sum_{j=1}^{i} U_j + V_j$. The number $n_1 \ge 0$ is define by relation $X_{n_1} - V_{n_1} < L \le X_{n_1}$ or $X_{n_1} < L \le X_{n_1} + V_{n_1+1}$.

3. If $n_1 > 0$ then ith irregularity $Z_i^{(1)}(x)$, $0 \le x \le L$, is set to be zero for x outside the interval $[X_i - V_i, X_i]$. For x in the interval $[X_i - V_i, X_i]$, the irregularity $Z_i^{(1)}(x)$ is a zero mean Gaussian process. The covariance $r(x, y)$ between $Z_i^{(1)}(x)$ and $Z_i^{(1)}(y)$ is defined by

$$r(x, y) = r_1(y - x) - R(x)\Sigma^{-1}R(y)^T$$

where $R(z) = [r_1(z + V_i - X_i + dx), r_1(z + V_i - X_i), r_1(z - X_i), r_1(z - X_i - dx)]$ while

$$\Sigma = \begin{bmatrix} r_1(0) & r_1(dx) & r_1(V_i + dx) & r_1(V_i + 2dx) \\ r_1(dx) & r_1(0) & r_1(V_i) & r_1(V_i + dx) \\ r_1(V_i + dx) & r_1(V_i) & r_1(0) & r_1(dx) \\ r_1(V_i + 2dx) & r_1(V_i + dx) & r_1(dx) & r_1(0) \end{bmatrix}.$$

4. The short wave irregularities $Z_i^{(2)}(x)$ are simulated independently using the steps given above with μ_1, θ_1 and r_1 replaced by μ_2, θ_2 and r_2, respectively.

5. Evaluate $Z(x) = Z_0(x) + \sum_{i=1}^{n_1} Z_i^{(1)}(x) + \sum_{i=1}^{n_2} Z_i^{(2)}(x)$ if $n_1 = 0$ or $n_2 = 0$ the sums are omitted.

LMA as a jump process

It is well known that the Laplace motion is a pure jump process, i.e. its increments are sums accumulating jump values only. Therefore, a LMA essentially represents the effects of shocks (impulses) due to these jumps filtered by the kernel function. Indeed the series expansion of a standard Laplace motion with parameter ν is given by

$$\Lambda(x) = \sum_{i=1}^{\infty} \sqrt{\nu} Z_i \left(e^{-\nu\gamma_i/L} W_i \right)^{1/2} \mathbf{1}_{(0,x]}(U_i), \quad 0 \le x \le L,$$

where W_i are i.i.d. standard exponential variables independent of $\{\gamma_i\}$ and $\{U_i\}$, Z_i's are independent standard Gaussian variables, γ_i is a location of the i-th point in a Poisson process, i.e. $\gamma_i = \sum_{j=1}^{i} G_j$,

where G_j are independent standard exponential distributed random variables. Finally U_i are independent uniformly on $[0, L]$ distributed random variables, cf. [7], [1].

Consequently, the LMA $Z(x)$ in (5) is given by the following series expansion

$$Z(x) \approx \int_0^L f(x-u)\, d\Lambda(u) = \sum_{i=1}^{\infty} \sqrt{\nu}\, X_i \left(e^{-\nu\gamma_i/L} W_i\right)^{1/2} f(x-U_i) = \sum_{i=1}^{\infty} Z_i(x). \tag{12}$$

Note that in average the terms $Z_i(t)$ are decreasing with i and the variances form a geometric series

$$\mathsf{V}\left[Z_i(x)\right] = \frac{\nu}{L}\left(\frac{L}{L+\nu}\right)^i \int_0^L f^2(x-u)\, du.$$

From this we observe that

$$\mathsf{V}\left[\sum_{i=1}^{\infty} Z_i(x)\right] = \sum_{i=1}^{\infty} \mathsf{V}\left[Z_i\right] = \int_0^L f^2(x-u)\, du \approx 1,$$

where approximation is valid if x is not in the proximity of either 0 or L. Moreover,

$$\begin{aligned} \mathsf{V}\left[\sum_{i=N+1}^{\infty} Z_i(x)\right] &= \int_0^L f^2(x-u)\, du \frac{\nu}{L} \sum_{i=N+1}^{\infty} \left(\frac{L}{L+\nu}\right)^i \\ &= \int_0^L f^2(x-u)\, du \left(1 - \frac{\nu}{L+\nu}\right)^N \\ &\approx e^{-\nu N/L}, \end{aligned} \tag{13}$$

where the approximation is for L and N large and x is not in the proximity of either 0 or L.